International Journal of Scientific Engineering and Applied Science (IJSEAS) – Volume-7, Issue-8, August 2021
ISSN: 2395-3470
www.ijseas.com

AHP and GIS Approach for Evaluating Landslide Vulnerability in the Lumbay Watershed, Guindulman, Bohol

Marne G. Origenes and Renato L. Lapitan

Graduate School, University of the University of the Philippines-Los Baños

Institute of Renewable and Natural Resources, College of Forestry and Natural Resources

University of the Philippines-Los Baños, Los Baños, Laguna

Abstract: Landslides are one of the natural hazards that can have a negative impact on people's lives. The purpose of this study was to evaluate how each vulnerability map differed when created using different methodologies for assessing overall landslide vulnerability of the Lumbay watershed. It has been demonstrated that GIS-based techniques combined with AHP can assess landslide vulnerability in a watershed while taking physical and anthropogenic factors into account. Furthermore, the slope, rainfall, and road distance obtained the highest weights, indicating that these elements play a role in landslide incidence in the watershed area. The landslide inventory map revealed that the modelled maps are extremely reliable, with 57%, 63%, and 55% of landslides and any sort of mass movement occurrences detected in high vulnerability classes of the vulnerability map produced. In this regard, the accuracy using the confusion matrix on the map produced using AHP combined with the WOM with >300mm rainfall data demonstrated the highest accuracy of 100% when compared to the other techniques. Both approaches indicated that the obtained results are scientifically correct however, as with the other studies, the highest accuracy must be selected and used for the recommendation of various strategies to lessen the impact of this hazard. Moreover, it was observed that density of landslides was mostly distributed in grassland cover areas and could be found in less than 100 meters from the road. As a result, adequate action is essential to prevent landslides from occurring, necessitating the development of rules and regulations in the watershed area to limit such effects.

Keywords: Landslide, AHP, WOM, raster calculator, accuracy, confusion matrix

I. Introduction

Landslides are one of the most common natural disasters in mountainous areas and are regarded as the greatest threat in a large number of regions around the world, putting people's lives and property at risk (Chakraborty et al., 2012; Goetz et al., 2011; Regmi et al., 2014; Pourghasemi et al., 2013). It is caused by a number of factors, making it difficult to analyze and predict (Mahalingam et al., 2016). Furthermore, the damages caused by landslides are expected to increase in the coming decades due to population growth, the progression of residential areas and infrastructure in high-risk areas, ongoing deforestation, and an increase in regional precipitation (Regmi et al., 2014). As a result, it is necessary to examine the conditions under which landslides have occurred in the past and to use critical combinations of preparatory factors to delineate the possibility of future landslides.

Preston et al. (2011) emphasize the importance of mapping the degree of vulnerability in order to produce and represent local context scenarios. One of the primary approaches for developing hazard reduction strategies is to conduct a landslide vulnerability assessment using geographic information system (GIS) analysis, which provides a powerful tool for modeling landslide hazards (Dai et al., 2002; Cevik and Topal, 2003; Ayalew and Yamagishi, 2005; and Fall et al., 2006) and based on expert judgment, the Analytic Hierarchy Process (AHP) tool was deemed to be a suitable tool for collecting and analyzing vulnerability, as well as for conducting an effective and context-specific vulnerability assessment (Nghiem, 2015), which is particularly suited to decisions made with limited information (Saaty et al. 2001).

Meanwhile, landslides are a common hazard in the Lumbay watershed during the rainy season. Hence, the primary purpose of this study is to determine how each vulnerability map differs when constructed using various approaches for estimating overall landslide vulnerability. Because different methods produce different study results, the modifications will tell us which method is fairly applicable to the watershed. The study concentrated on the integration of AHP and GIS-based methods while taking into account the physical and anthropogenic factors influencing the watershed's vulnerability. Another goal is to identify landslide occurrences and the degree of landslide vulnerability in order to evaluate the performance of these models using a confusion matrix. The main research gap in this study is a lack of comprehensive information at the watershed level, and it will only use what is available. Thus, the primary goal of this study was to investigate and determine the differences between the methods used to generate the landslide vulnerability assessment of the Lumbay watershed, a potential hotspot area for landslide occurrences, in order to manage natural resources and reduce losses in the future.

II. Materials and Methods

Study area

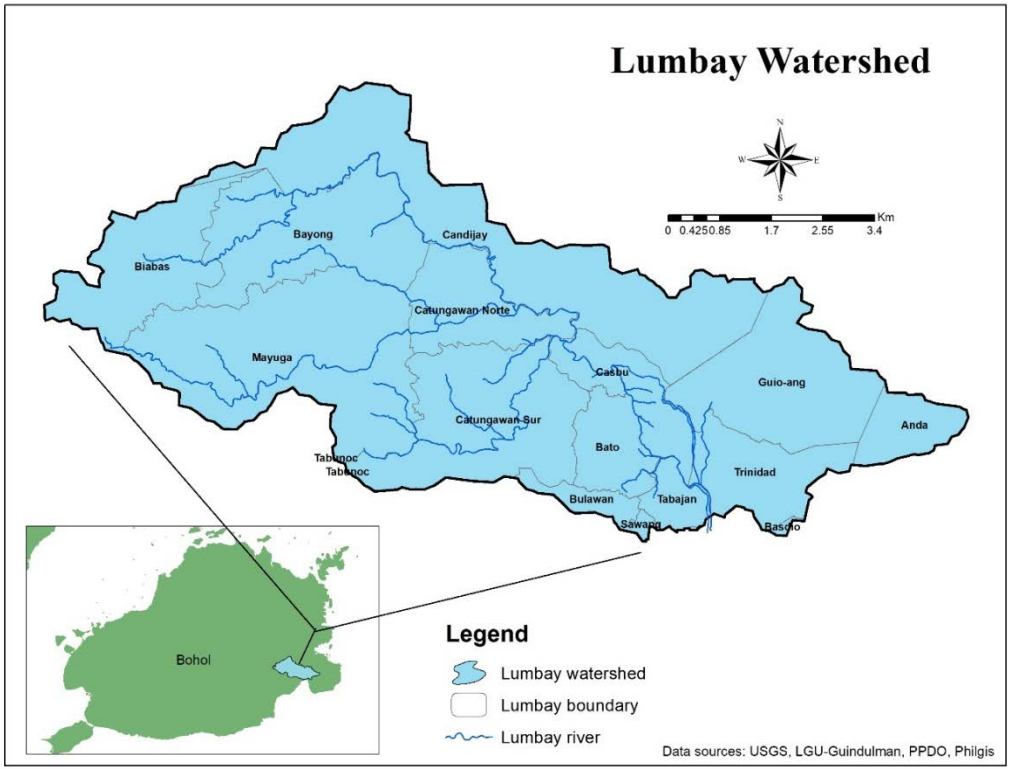

Figure 1. Location of map of the study

The Lumbay watershed lies in the coastal municipality of Guindulman in the province of Bohol with geographic coordinates of 9°44'20" and 9°48'40" North latitude, and 124°25' E to 124°31'30" East longitude. The watershed covers a total area of 5,461 hectares (generated from a 30m x 30m DEM) and includes the municipalities of Guindulman (78.62%), Candijay (18.64%), and Anda (2.74%).

According to PAG-ASA, the Lumbay watershed is under Corona's fourth (4th) Type zone. This category comprises places where there is more or less uniformly distributed year-round rainfall or where there is heavy rainfall for the majority of the year with only a brief dry season. The average monthly rainfall data of the watershed ranged between 100mm – 200mm (based on data from the power.larc.nasa.gov website) and >300mm (downloaded from worldclim.com).

The watershed comprised of less than 8% (level to undulating), followed by 30% to 50% (steep) in slope and the elevation ranges from 1 to 610 meters above sea level (masl).

Datasets and sources

The current study relied on secondary data gathered from a variety of sources. These included the 5m x5m Digital Terrain Model (DTM) and land cover obtained from NAMRIA. Rainfall data was generated by BSWM from the power.larc.nasa.gov website, and rainfall was downloaded from the worldclim.com website. Geology was downloaded from the Philgis.org website, soil map sourced out from BSWM; provincial boundary from PPDO, municipal and barangay boundary from LGU-Guindulman from NAMRIA; road network obtained from LGU-Guindulman; land use and stream network digitized from PPDO and built-ups downloaded and digitized from OSM and Google Earth images.

The boundary of Lumbay watershed was created using 30m x 30m cell size resolution downloaded from USGS.

Generation of spatial maps using GIS

The landslide vulnerability due to physical factors were slope, rainfall, land cover, soil and geology. While the anthropogenic factors were NPAAAD (alternative to farming system), distance to road, river and built-ups areas. The vector files of these maps were converted to a raster file format with a 5m x 5m resolution, and then reclassified based on Table 1. Proximity to roads, built-ups areas and rivers was classified into five different buffer categories using a Euclidean distance interpolation method in the GIS application and reclassified into five classes (e.g. <100, 100-200m, 200-300m, 300-500m and >500m for very low). These maps were classified into different classes according to the requirement using the natural breaks (Jenks) method. All maps were processed and georeferenced using ArcGIS 10.7 using projected Universal Transverse Mercator (UTM-51N) and Luzon 1911 UTM Zone 51N.

All thematic maps were transformed to hazard class rating maps based on the procedure contained in the ERDB Manual for Vulnerability Assessment (ERDB, 20011). The following hazard categories were assigned to the factors: the levels are 1–Very Low, 2–Low, 3–Moderate, 4–High, and 5–Very High (see Table 2)

Table 1. Rating of physical factors affecting Landslide

Vulnerability Class	Class/ Rating	Slope (%)	Rainfall (mm)	Land cover	Soil Type	Geology
Very Low	1	< 8%	< 100mm	Mangrove forest; Inland water; Fishpond	-	Upper Miocene-Pliocene (Sedimentary & Rocks)
Low	2	8.1-18%	100.1-200mm	open forest	Ubay Clay	Pliocene-Pleistocene
Moderate	3	18.1-30%	200.1-300mm	Brush/shrubs, built-ups; Grassland	Bolinao Clay	Cretaceous - Paleogene
High	4	30.1-50%	300.1-500mm	Perennial crops, Annual crops,	Mountain Soil (Undifferentiated)	Upper Miocene - Pliocene (N2)
Very High	5	>50%	> 500mm		-	Recent (R)

Table 2. Vulnerability class

Vulnerability Class	Rating
Very Low Vulnerability	< 2.1
Low Vulnerability	2.1 – 2.79
Moderately Vulnerable	2.8 – 3.49
Highly Vulnerable	3.5 – 4.19
Very Highly Vulnerable	>4.2

Vulnerability factors equations

Physical and anthropogenic factors were assigned numerical scores based on their relative importance in influencing landslides. The overall landslide vulnerability map was created by adding the physical and anthropogenic factors together. The following is the mathematical model used to calculate overall landslide vulnerability:

Physical factors

$$V_{Lp} = S\ (29.9) + R\ (27.1) + Lc\ (14.6) + St\ (14.8) + G\ (13.6) \quad (1)$$

Where: S = slope; R = rainfall; Lc = land cover; St = soil type; G = geology

Anthropogenic factors

$$V_{La} = NPAAAD\ (25.8) + road\ distance\ (63.7) + built\text{-}up\ distance\ (10.5) / 3 \quad (2)$$

Where: NPAAAD = network of protected area for agriculture and agro-industrial development

Overall landslide vulnerability

$$V_L = V_{Lp}\ (66.7) + V_{La}\ (33.3) \quad (3)$$

V_{Lp} = vulnerability due to physical factors;
V_{La} = vulnerability due to anthropogenic factors

AHP Analysis

In this study, the AHP method for weighting the criteria of physical and anthropogenic factors and calculate its overall vulnerability affecting the landslide vulnerability of the watershed was computed. The relative ranking of each pair of factors was guided by the knowledge of local experts. This method involves performing a pairwise comparison of all possible pairs of factors and attempting to synthesize the judgments to determine the weights (Saaty, 2001). In matrix-based pair-wise comparison, if the factor on the horizontal axis is more important than the factor on the vertical axis, this value ranges between 1 and 9. In contrast, the value varies between the reciprocals 1/2 and 1/9 (Table 3). The consistency ratio (CR) was calculated to assess the consistency of comparisons in the pairwise comparison matrix. If the value is equal to or less than 0.1, the CR is considered acceptable (Malczewski, 2010). The CR is obtained by comparing the consistency index (CI) with average random consistency index (RI). Otherwise, a reassessment of the provided qualitative judgment and recalculation of weights is required. The CR was computed using the following equation:

$$CR = \text{Consistency Index/Random Index}, \quad (4)$$

where random index (RI) denotes the randomly generated average consistency index and consistency index (CI) is defined as follows (see Table 4):

$$CI = (\lambda max - n)/(n - 1), \quad (5)$$

where λmax represents the largest eigenvalue of the matrix and n refers to the order of the matrix (Mahapatra et al., 2015).

The calculations were carried out using the AHP online tool developed by Goepel (2018).

Table 3. Scale of relative importance between two predictive factors (Saaty, 1980)

Intensity of Importance	Definition	Explanation
1	Equal importance	Two factors contribute equally to the objective
3	Moderately more important	Experience and judgment slightly to moderately favor one activity over another
5	Strongly important	Experience and judgment strongly or essentially favor one activity over another
7	Very strongly important	An activity is strongly favored over another and its dominance is showed in practice
9	Extremely more important	The evidence of favoring one factor over another is of the highest degree possible of an affirmation
2, 4, 6, 8	Intermediate values	Used to represent compromises between the references in weight 1, 3, 5, 7, and 9
Reciprocals	Opposites	Used for inverse comparison

Table 4. Average random consistency index (RI)

N	2	3	4	5	6	7	8	9	10
λ_{max}	0	0.58	0.90	1.12	1.24	1.32	1.41	1.45	1.49

GIS analysis tools

Weighted overlay method (WOM)

The weighted overlay technique is used to create a map by overlaying several raster layers and assigning weight to each raster layer based on its importance (Saaty, 1990). Weights are assigned to each raster layer both externally and internally based on their relative importance as determined by expert opinion. External weights or weight values refer to the total weights of all layers, which must be equal to 100, whereas internal weights or rating values are referred to as class values (class 1-5). AHP was used to compute the weight values and rating values of each event-controlling factor. Following the assignment of weights to the model, all raster layers were added to the weighted overlay tool for analysis. Finally, landslide vulnerability map was created using the weighted overlay method in ArcGIS software. The outcomes of this activity include the identification of vulnerable areas as well as the classification (from high to low) of various hazards (degree of vulnerability). All layers were combined by using the weighted overlay tool based on Equation (6):

$$S = \frac{\sum W_i S_{ij}}{\sum W_i}, \qquad (6)$$

where *Wi* is the weight of *i* th factor, *Sij* represents subclass weight of *j* th factor and *S* is the spatial unit of the final map.

Raster calculator tool

Each raster layer of physical and anthropogenic factors with weighted information content was multiplied by its weight (obtained using the AHP analysis method), and the single factor layers with weighted information contents were overlain using the ArcGIS raster calculator tool, resulting in an overall landslide vulnerability map using equations 1, 2, and 3.

Landslide inventory map and accuracy assessment

The landslide validation map was created using the actual location of the landslide. The geographic coordinates of the landslide were taken, refined in Google Earth Pro, and converted to a GIS-compatible format. A field visit was conducted in March – April 2021 to assess the accuracy of the landslide vulnerability map produced in this study. The field visit included identifying where landslides and any type of mass movement (Guzzetti et al., 2012) were observed within the watershed area.

The accuracy assessment is required to validate the performance of the vulnerability map produced by the weighted overlay method and the raster calculator tool. Two types of accuracy evaluation were obtained in this study. First, map classes were compared to landslide densities in those classes. The known location of the landslide was compared and overlaid with the vulnerability map generated by AHP and various GIS methods. The analysis was based on the study of Basharat et al. (2016) showing spatial analysis between landslide events and vulnerability maps. The accuracy assessment was calculated by dividing the number of verified landslide locations from the inventory map over the total number of landslide locations collected during field surveys. The distribution of these landslide events was calculated in all classes of the vulnerability map. If the majority of the landslide events fall within the high and very high vulnerability classes, this indicates a good agreement. On the other hand, if the majority of the

landslide events fall within the low and moderate vulnerability classes, this indicates a low accuracy rate. The second step in calculating accuracy is to compare the Lumbay watershed's landslide vulnerability map with the landslide inventory map, with the percentage of overlap between the two indicating how well the model predicts reality. The model was compared to the landslide inventory using the study to determine overall accuracy (calculated by the total number of correctly classified pixels of landslides and non-landslides divided by the total number of pixels or landslides in the study area) (Miandad et al., 2020). Accuracy were calculated using a cross table that depicts the amount of overlap and relationship between inventory and predicted maps.

III. Results and Discussion

Analytic Hierarchy Process (AHP) analysis

Table 5. Pairwise comparison matrix, weight and consistency ratio of landslide vulnerability factors

Physical Factors	**Slope**	**Rainfall**	**Land Cover**	**Soil**	**Geology**	**Weights**
Slope	**1**	1	3	2	2	29.9 %
Rainfall	1	**1**	3	1	2	27.1 %
Land Cover	0.33	0.33	**1**	2	1	14.6 %
Soil	0.50	1	0.50	**1**	1	14.8 %
Geology	0.50	0.50	1	1	**1**	13.6 %
			CR = 8.6 %			
Anthropogenic Factors	**NPAAAD**	**Road Distance**	**Built-up Distance**			**Weights**
NPAAAD	**1**	0.33	3			25.8 %
Road Distance	3	**1**	5			63.7 %
Built-up Distance	0.33	0.20	**1**			10.5 %
			CR = 0.4 %			
Overall Factors	**Physical Factors**		**Anthropogenic Factors**			**Weights**
Physical Factors	**1**		2			66.7%
Anthropogenic Factors	0.50		**1**			33.3%
			CR = 0%			

The AHP was used to estimate the weights and ratings for vulnerability factors: physical and anthropogenic factors, both of which can be obtained from the pairwise comparison matrix. As shown in Table 5, slope and rainfall were the most influential physical factors, with a value of 29.9% and 27.1%, respectively. The factors soil, land cover, and geology were deemed less important due to a lack of information and the difficulty in identifying these factors affecting the vulnerability of the watershed. On the other hand, in terms of anthropogenic factors, road distance obtained the highest weights. Road distance, on the other hand, received the highest weights in terms of anthropogenic factors. Furthermore, physical factors received the highest weights in the overall factors, with a value of 66.7%. This value was assigned because the majority of the landslides in the watershed area were located in road areas, which are classified as man-made.

Additionally, the CR values were less than 10% (Table 5), which corresponds to the consistency of the pairwise comparison. As a result, these findings validate the ratings and weights of the factors (Pourghasemi et al., 2012).

Overall, slope, rainfall, and road distance were the most important vulnerability factors influencing landslide distribution as determined by AHP pairwise comparison.

Vulnerability Factors

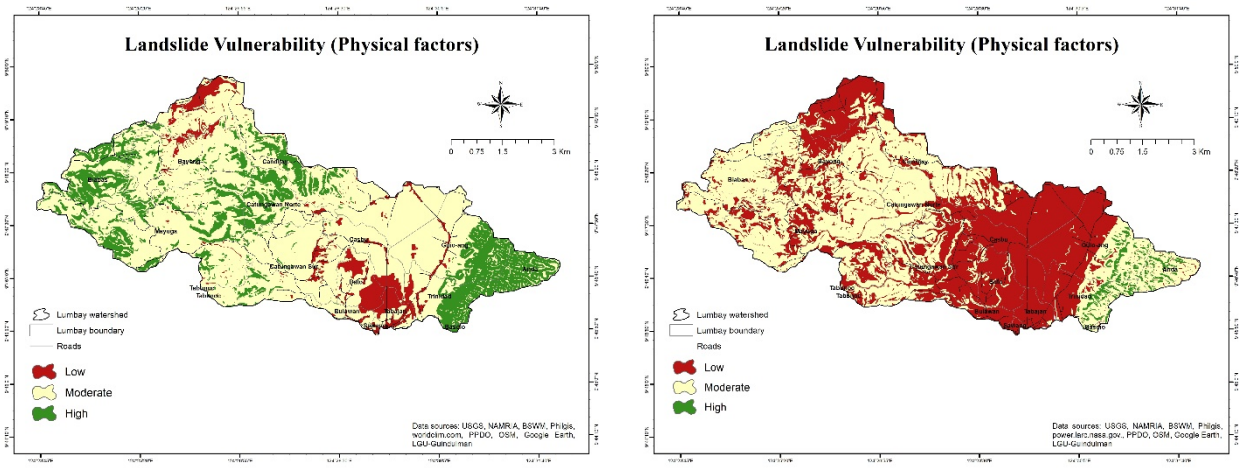

Figure 2. Landslide vulnerability due to physical factors using weighted overlay method
a) >300mm RF; b) 100-200mm RF

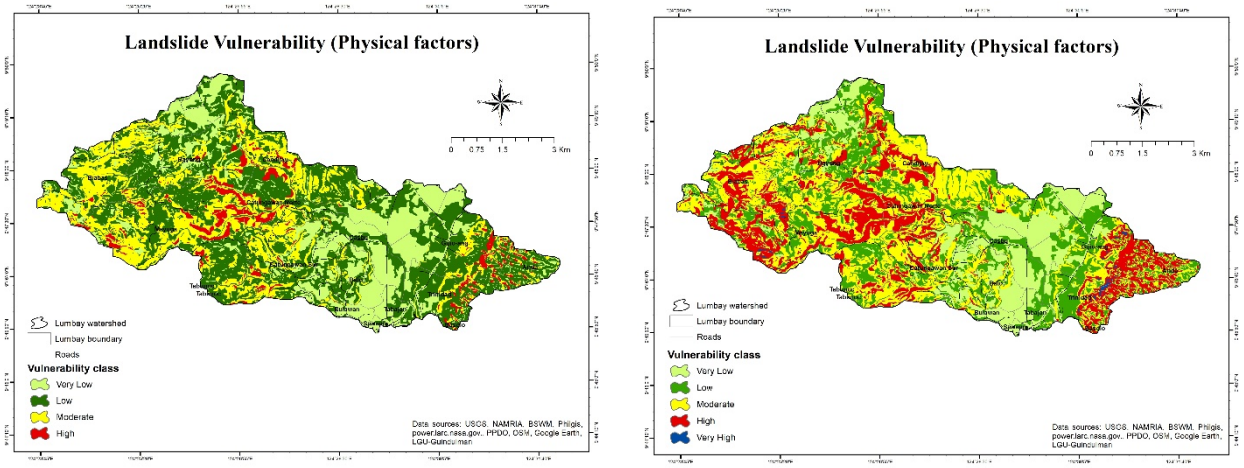

Figure 3. Landslide vulnerability due to physical factors using raster calculator tool
a) >300mm RF; b) 100-200mm RF

Anthropogenic factors

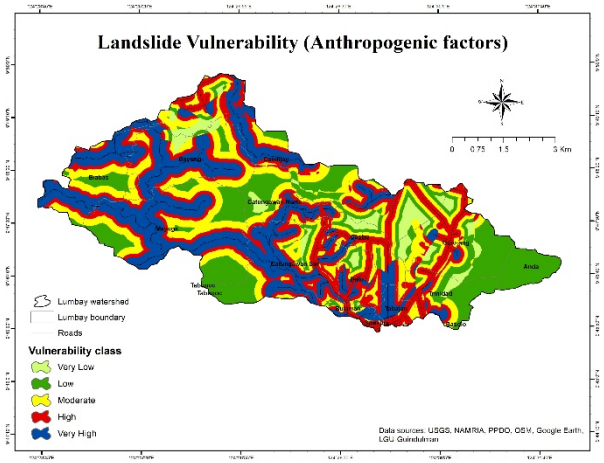

Figure 4. Landslide vulnerability due to anthropogenic factors

Figure 2 illustrates the landslide vulnerability due to physical factors using >300mm rainfall (Fig. 2a) and rainfall ranging from 100mm-200mm (Fig.2b). As a result, physical factors were integrated into the GIS environment using a WOM, and each factor was multiplied by its assigned weight created by AHP pairwise comparison to generate the landslide vulnerability map (physical factors).

Figure 3 depicts the landslide vulnerability (physical factors) using the raster calculator tool. Accordingly, several physical factors were integrated into the GIS environment using a raster calculator tool, and each factors was multiplied by its assigned weight to generate the landslide vulnerability map (physical factors) as shown in Equation (1).

The landslide vulnerability due to anthropogenic factors is illustrated in Figure 4. The calculation was modified in accordance with the ERDB vulnerability assessment manual (2011). However, as an alternative to the farming system, the Network of Protected Areas for Agriculture and Agro-Industrial Development (NPAAD) was used and calculated using equation (2).

Local experts assigned the greatest weight to road distance because several landslides in the area were frequently discovered adjacent to the road.

Overall Landslide Vulnerability

The vulnerability map was classified based on Table 2 to obtain the overall landslide vulnerability, which was calculated by combining physical and anthropogenic factors. Figure 5 shows the overall landslide vulnerability maps were based on physical factors calculated using WOM and anthropogenic factors calculated using equation (2).

Each single vulnerability factor (physical factor) was multiplied by its weight (obtained using the AHP method) with the weighted information content of the landslide vulnerability assessment model for Lumbay watershed, resulting in an overall landslide vulnerability map, as shown in Figure 5a & b. According to the results in Figure 5a, a large portion of the watershed (60%) is moderately vulnerable to landslides, 22.85% is high to very highly vulnerable, and only 18% is low to very low vulnerable. Figure 5b shows that 44% of the watershed is moderately vulnerable, 8.54% is high to very highly vulnerable, and 47% is low to very low vulnerable to

landslides. The results showed that the road area with steeper slopes was highly to very highly vulnerable to landslides.

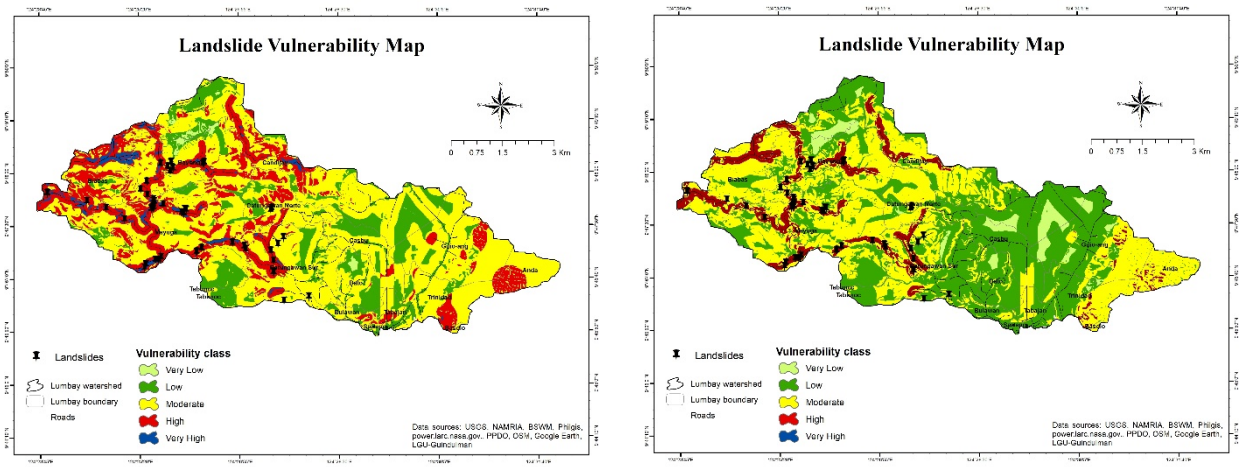

Figure 5. Overall landslide vulnerability using weighted overlay method a) >300mm RF; b) 100-200mm RF

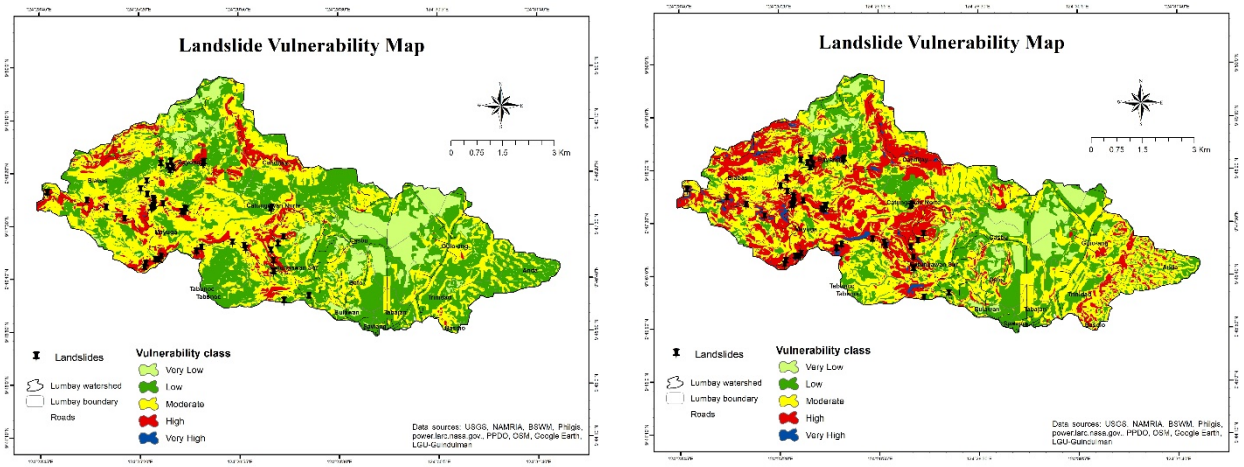

Figure 6. Overall landslide vulnerability using raster calculator tool a) >300mm RF; b) 100-200mm RF

The overall landslide vulnerability maps were generated using the raster calculator tool (physical factors) and the anthropogenic factors (calculated using equation 2) (Figure 6). Based on the results in Figure 6a, a large percentage of the watershed (41%) is low vulnerability to landslides, followed by very low vulnerability (11%), and only 8% is high to very high vulnerability to landslides. According to Figure 6b, 44% of the watershed is moderately vulnerable, 23% is high to very highly vulnerable, and only 33% is low to very low vulnerable to landslides. To generate the landslide vulnerability map, the raster layer of each physical and anthropogenic factor is multiplied by their given weights using the raster calculator tool and summed together using the weighted sum overlay tool in GIS, as shown in Figure 6. The results show a significant difference between the outcomes of Figures 6a and 6b.

In this study, the AHP and GIS-based methods were used to generate predictive landslide vulnerability maps for the Lumbay watershed using two different rainfall data sets and two GIS tools. The vulnerability maps were created based on the physical and anthropogenic factors affecting the watershed. The GIS approach validated the capability of GIS technology in assessing landslide vulnerability. Based on the findings of this study, it is possible to conclude that the high and very high vulnerability landslide zones identified by the AHP method can predict potential landslide areas in the real world. The AHP can be used to evaluate the relative performance of decision alternatives with respect to the relevant criteria. According to Saaty et al. (2001), AHP was seen to be a suitable tool and is particularly suited to decisions made with limited information. The study's findings indicate that when field conditions are properly determined by good proficiency, the AHP method can produce more truly good results (Moradi et al., 2012). AHP is a simple and easy way to rate various factors affecting landslide vulnerability. The CR value remained below 10%, indicating appropriate and reliable weighting criteria. Despite the fact that the AHP-based model has drawbacks due to its subjective approach, AHP is a very useful tool for comparing different factors.

The most important vulnerability factors controlling the landslide distribution derived from AHP pairwise comparison were slope, rainfall, and road distance, which were considered basic conditions for slope stability. This is in agreement with the study of Derbyshire et al. (2001), which found that the road network has the greatest influence on the spatial distribution of landslides. This is due to uncontrolled blasting and excavation during road construction on these fragile slopes, which causes frequent landslides (Devkota et al., 2013). This is also true in the study of Nohani et al. (2019), who discovered that poor road construction is one of the most effective determinants of landslide occurrence. According to Coco and Buccolini (2015), in the same geological and climatic setting, slope is an important driving parameter for slope failures. The shear strength decreases as the slope increases. As a result, the density of landslides increases as the steepness of the slope increases (Pradhan et al., 2010). According to Kartiko et al. (2006), more than half of all landslides occur in areas with slopes greater than 25%.

There are many models developed for landslide vulnerability and susceptibility, according to Nohani et al. (2019), but there are no universal guidelines for model selection to model a better landslide vulnerability assessment. Meanwhile, preparing for landslide vulnerability is one of the most practical approaches for landslide hazard assessment and proper management tasks (Guzzetti, 2006). The present study therefore will help in providing better choices on what specific approach or technique to be used in landslide vulnerability assessment with emphasis on having a higher accuracy.

Landslide density

The results clearly show that the density of landslide events increases with grassland cover (53%), then with perennial crops (24%), 10% for annual crops and brush/shrubs land and built-up areas (6%) (Figure 7a). Vegetation is important in increasing slope stability and decreasing landslide susceptibility (Miles and Keefer, 2007). Therefore, grassland cover is incapable of stabilizing the slope, increasing the risk of landslides in the watershed area.

Meanwhile, the density of landslide events increases in less than 100 meters of road distance (Figure 7b). As a result, the likelihood of a landslide increases as the distance from the road decreases. This means that proper action should be taken to prevent such hazard from occurring in the road area.

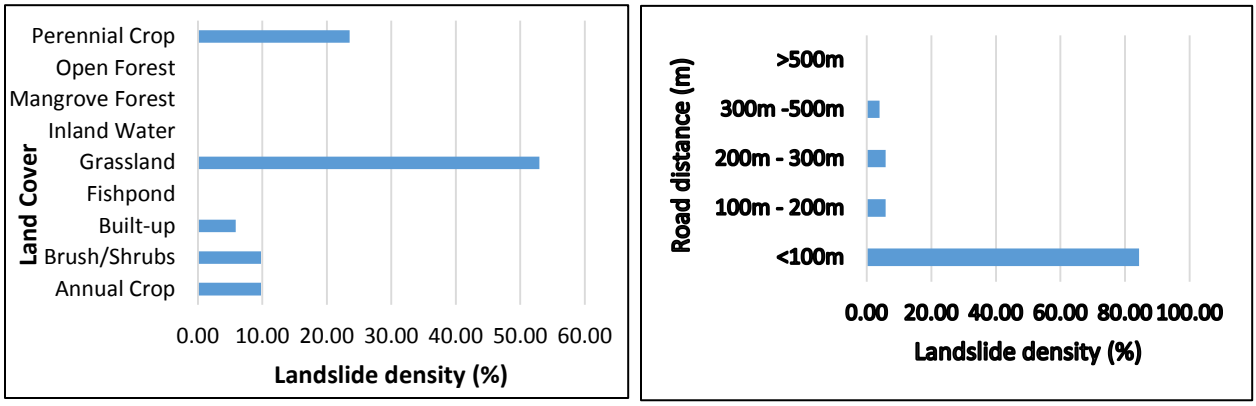

Figure 7. Landslide density: a) Land cover map and b) road distance

Landslide inventory

Table 6. Overlaid landslide events in the vulnerability map produced using weighted overlay method

a) Rainfall: >300mm		b) Rainfall: 100 – 200mm	
Vulnerability class	Landslide percentage (%)	Vulnerability class	Landslide percentage (%)
		Low	6
Moderate	16	Moderate	31
High	**57**	High	**63**
Very High	27		
Total	**100%**		**100%**

Table 7. Overlaid landslide locations in the vulnerability map produced using raster calculator tool method

a) Rainfall: >300mm		b) Rainfall: 100 – 200mm	
Vulnerability class	Landslide percentage (%)	Vulnerability class	Landslide percentage (%)
Low	14	Low	12
Moderate	**53**	Moderate	27
High	33	High	**55**
		Very High	6
Total	**100%**		**100%**

The most crucial and fundamental data set is the landslide inventory. The study created and used a landslide inventory by validating the actual location of landslide occurrences and any type of mass movement. Thus, the extent of landslides was not included because it is inaccessible, not feasible, and also for the researcher's safety.

Table 6 shows the overlaid landslide events or any mass movement to the vulnerability map created with WOM and two different rainfall datasets. According to the findings, landslide events are mostly found in the highly vulnerable (57%) and very highly vulnerable (27%)

categories, with the remaining 16% falling into the moderate vulnerability category (Table 6a). Conversely, 63% of landslides and any mass movement inside the watershed were identified in the highly vulnerable category, followed by 30% in the moderate category, and the remaining 6% in the low vulnerability category (Table 6b).

Landslide events or any type of mass movement were overlaid on the vulnerability map created with the raster calculator tool. The findings show that landslide events were common in the moderately vulnerable (Table 7a) and highly vulnerable (Figure 7b) classes, with percentage values of 53% and 55%, respectively.

The majority of the landslide events were found in high vulnerability areas, with very few landslides found in moderate to low vulnerability classes (Table 6a, b & 7b). Based on the methods of this study, if the majority of the landslide events fall into the high and very high vulnerability classes, this indicates good agreement. Therefore, the values of 57%, 63%, and 55% (Tables 6a, b, and 7b) support the existence of a strong link between vulnerability classes and landslide events. As a result, this assessment indicates that the map is accurate enough. However, if the majority of landslide events fall into the low and moderate vulnerability classes, this indicates a low accuracy rate. As a result, 53% of landslides are classified as moderately vulnerable, indicating a low accuracy rate (Table 7a).

Accuracy assessment using confusion matrix

Table 8. Confusion matrix of landslide inventory and vulnerability map (WOM)

a) Rainfall: >300mm				**b) Rainfall: 100 – 200mm**			
		Reference data				Reference data	
		With landslide	No landslide			With landslide	No landslide
Classified data	With landslide	**51**	0	Classified data	With landslide	**48**	0
	No Landslide	0	**0**		No Landslide	3	**0**
Overall accuracy		**100%**		**Overall accuracy**		**94.12%**	

Table 9. Confusion matrix of landslide inventory and vulnerability map (raster calculator tool)

a) Rainfall: >300mm				**b) Rainfall: 100 – 200mm**			
		Reference data				Reference data	
		With landslide	No landslide			With landslide	No landslide
Classified data	With landslide	**44**	0	Classified data	With landslide	**42**	0
	No Landslide	7	**0**		No Landslide	6	**0**
Overall accuracy		**86.27%**		**Overall accuracy**		**82.35%**	

Table 8 shows the confusion matrix of landslide inventory and vulnerability map produced based on WOM. Based on the results, fifty one (51) of the landslide events in the inventory were correctly matched in the classified data. Therefore, it achieved a total accuracy of 100% (Table 8a). In contrast, only forty eight (48) landslide locations were correctly classified out of 51 landslide events, with three (3) misclassified, yielding an overall accuracy of 94.12% (Table 8b).

Table 9 displays the confusion matrix of the landslide inventory and vulnerability map generated using the raster calculator tool. The results show that only forty four (44) landslide locations were correctly classified, and only seven (7) were misclassified in the classified data using >300mm of rainfall data, yielding an overall accuracy of 86.27% (Table 9a). Table 9b, on the other hand, shows that only forty two (42) landslide events were correctly classified, yielding an overall accuracy of 82.35%.

In general, the validation was based on the actual location of the landslide and any type of mass movement, such as soil creep, in the watershed areas. Most landslides in the Lumbay watershed are caused by soil creep, which is common in grassland areas and causes slope failure. It was frequently observed that grassland converted to houses was cracked and damaged, with visible creeps around the area. Furthermore, flows are one type of landslide, whereas creep is one of the categories of flows, and creep is defined as the imperceptibly slow, steady downward movement of slope-forming soil or rock by the USGS (2014). Moreover, the movement is caused by shear stress which is strong enough to cause permanent deformation but not strong enough to cause shear failure. However, because it was not included in the study, the study cannot conclude whether the type of creeps within the watershed are seasonal, continuous, or progressive.

According to Senouci et al. (2021), evaluating the quality of predictive landslide maps is a first step in this field. Two approaches were used in this study. The first method is based on the use of the landslide inventory map with the goal of overlaying it to the landslide vulnerability maps produced using the WOM and raster calculator tool. The quality of these maps was determined by comparing them to the landslide inventory map (Table 8 & 9). According to the findings, landslide locations were commonly observed in highly vulnerable to landslide areas using both methods, with the exception of >300mm rainfall calculated using the raster calculator tool (Table 9a). The second method employed the use of a confusion matrix, which is calculated by dividing the total number of corrected points or pixels by the total number of landslide location events (Miandad et al., 2020). The overall accuracy for the map based on AHP combined with WOM using >300 mm rainfall and 100mm-200mm rainfall was 100% and 94.12%, respectively. In contrast, the overall accuracy of maps computed using the raster calculator tool was 86.27% and 82.35%, respectively. These results indicate that the models used are appropriate for mapping landslide vulnerability. Thus, the landslide predictive maps produced acceptable results based on the techniques used in this study.

Conclusion

The danger of landslides have imposed enormous constraints on socioeconomic development (Senouci et al., 2021). Many approaches, including qualitative and quantitative approaches, have been tried for landslide assessment studies. In this study, a semi-quantitative method was used, as well as the analytical hierarchy process (AHP) and GIS-based analysis using various computation methods such as WOM and raster calculator tool. The study distinguished between the aforementioned methods and calculated their accuracy. GIS-based

methods, combined with the use of AHP, have demonstrated their ability to assess landslide vulnerability in a watershed. The use of AHP has provided a solid foundation for determining the relative significance of landslide vulnerability factors. According to the AHP results, the slope, rainfall, and road distance received the highest weights, indicating that these factors play a role in the occurrence of landslides in the watershed area.

A set of landslide vulnerability maps for the Lumbay watershed were created using two different GIS tools: WOM and raster calculator, with two different rainfall data sets: >300mm and 100mm-200mm. The final map was then subjected to five different classes of landslide vulnerability: very low, low, moderate, high, and very high vulnerability.

The predictive landslide vulnerability maps were evaluated using a landslide inventory map that depicted the location of landslides and other types of mass movement events in the area. Given the location of the landslide and any mass movement events, the landslide inventory map confirmed that the modelled maps have exceptional reliability showing 57%, 63%, and 55% were found in high vulnerability classes. Meanwhile, the confusion matrix based on different rainfall datasets and the GIS tool used with AHP shows a higher accuracy. The accuracy of the vulnerability maps produced in this study using the AHP combined with WOM is 100%, followed by 100mm-200mm rainfall using WOM (94.12%), >300mm rainfall using raster calculator (86.27%), and 82.35% for 100mm-200mm rainfall using raster calculator tool, which is very satisfactory. Both techniques demonstrated that the obtained results are scientifically correct. However, as with the other studies, a method with highest accuracy must be selected to be used for the recommendation of various measures to reduce the impact of landslide hazard.

Moreover, it was observed that the density of landslides based on land cover and road distance was mostly distributed in grassland cover areas and could be found less than 100 meters from the road. This means that proper intervention is required to prevent landslides from occurring, particularly during the rainy season.

The study suggested that a characterization of the watershed particularly its biophysical and socioeconomic aspects must be undertaken and carried out thoroughly. Previous landslide occurrences adjacent to roads must be monitored and recorded for future references. Besides, using updated thematic maps will yield more reliable results. However, some of the thematic layers used in this study were out of date, such as the land cover map, which was taken in 2015.

All the more, while the watershed area is not densely populated, local governments can mitigate the effects of landslides by implementing policies and regulations within the watershed area. Furthermore, now is the best time to put in place the necessary safeguards to prevent these hazards from occurring. The vulnerability maps could be used to track the spread of landslides and prevent natural disasters. In this regard, the landslide vulnerability map could assist decision-makers in better designing future construction projects and avoiding construction in highly vulnerable zones without proper mitigation assessment. Lastly, this study must be incorporated in the comprehensive forest/land use plan of the area to ensure the sustainable development of the watershed and its natural resources.

Literature cited

Ayalew, L., H. Yamagishi, H. Marui and T. Kanno. 2005. Landslides in Sado Island of Japan: Part II. GIS-based susceptibility mapping with comparisons of results from two methods and verifications, Eng. Geol., 81, 432–445, https://doi.org/10.1016/j.enggeo.2005.08.004

Basharat, M., H. R. Shah and N. Hameed. 2016. Landslide susceptibility mapping using GIS and weighted overlay method: a case study from NW Himalayas, Pakistan

Chakraborty, S., and R. Pradhan. 2012. Development of GIS based landslide information system for the region of East Sikkim. Int. J. Comput. Appl., 49, 5–9.

Cevik, E. and T. Topal. 2003, GIS-based landslide susceptibility mapping for a problematic segment of the natural gas pipeline, Hendek (Turkey). Environmental Geology, 44, pp. 949–962.

Coco, L. and Buccolini, M.: The Effect of Morphometry, Landuse and Lithology on Landslides Susceptibility: An Exploratory Analysis, IOS Press, 779–784, https://doi.org/10.3233/978-1-61499-580-7-779, 2015.

Dai, F.C., C.F. Lee, and Y.Y. Ngai. 2002. Landslide risk assessment and management: an overview. Eng Geol 64:65–87

Derbyshire, E., M. Fort, and L.A. Owen. 2001. Geomorphological hazards along the Karakoram Highway: Khunjerab Pass to the Gilgit River, northernmost Pakistan, Erdkunde, 55, 49–71, https://doi.org/10.3112/erdkunde.2001.01.04

Devkota, K.C., A.D. Regmi, H.R. Pourghasemi, K. Yishida, B. Pradhan, I.C. Ryu, M.R. Dhital, O.F. Althuwaynee. 2013. Landslide susceptibility mapping using certainty factor, index of entropy and logistic regression models in GIS and their comparison at Mugling–Narayanghat road section in Nepal Himalaya. Nat. Hazards 65, 135–165

Dai, F.C. and C.F. Lee. 2002, Landslide characteristics and slope instability modelling using GIS, Lantau Island, Hong Kong. Geomorphology, 42, pp. 213–228.

ERDB (Ecosystem Research and Development Bureau). 2011. Manual on vulnerability assessment of watersheds. ERDB, Department of Environment and Natural Resources, College, Laguna

Fall, M., R. Azzam, and C. Noubactep. 2006. A multi-method approach to study the stability of natural slopes and landslide susceptibility mapping. Eng. Geol., 82, 241–263.

Goepel, K. D. 2018. Implementation of an Online Software Tool for the Analytic Hierarchy Process (AHP-OS). *Proceedings of the International Symposium on the Analytic Hierarchy Process: The 15th ISAHP Conference. Publication Date: July 2018.* http://dx.doi.org/10.13033/isahp.y2018.029

Goetz, J.N., R.H. Guthrie, and A. Brenning. 2011. Integrating physical and empirical landslide susceptibility models using generalized additive models. Geomorphology, 129, 376–386.

Guzzetti, F. 2006. Landslide Hazard and Risk Assessment. Ph.D. Thesis, University of Bonn, Bonn, Germany,

Guzzetti, F., A.C. Mondini, M. Cardinali, F. Fiorucci, M. Santangelo, and K.T. Chang. 2012. Landslide inventory maps: New tools for an old problem, Earth-Sci. Rev., 112, 42–66, https://doi.org/10.1016/j.earscirev.2012.02.001,

Kartiko, R. D., Brahmantyo, B., and Sadisun, I. A.: Slope and Lithological Controls on Landslide Distribution in West, in: International Symposium on Geotechnical Hazards: Prevention, Mitigation and Engineering Response, Utomo, Tohari, Murdohardono, Sadisun, April 2006, Yogyakarta, Indonesia, 177–184, 2006.

Mahalingam, R., Olsen, M.J. and O'Banion, M.S. 2016. Evaluation of landslide susceptibility mapping techniques using lidar-derived conditioning factors (Oregon case study), Geomatics, Natural Hazards and Risk, 7:6, 1884-1907, DOI:10.1080/19475705.2016.1172520

Mahapatra, M., R. Ramakrishnan, and A.S. Rajawat, 2015. Coastal vulnerability assessment using analytical hierarchical process for South Gujarat coast, India. Nat. Hazards, 76, 139–159.

Malczewski, J. 2010. Multiple Criteria Decision Analysis and Geographic Information Systems. In Trends in Multiple Criteria Decision Analysis; Ehrgott, M., Figueira, J.R., Greco, S., Eds.; Springer: New York, NY, USA,; Volume 142, pp. 369–395.

Miandad, J., M.M. Darrow, M.D. Hendricks, and R.P. Daanen. 2020. Landslide mapping using multiscale LiDAR digital elevation models. Environmental and Engineering Geoscience, 26(4), 405–425. https://doi.org/10.2113/eeg-2268

Miles, S.B., and D.K. Keefer. 2007. Comprehensive Areal Model of Earthquake-Induced Landslides: Technical Specification and User Guide; Open File Report; USGS: Reston, VA, USA,

Moradi M., M.H. Bazyar and M. Zargham. 2012. Journal of Basic and Applied Scientific Research, 2(7), 6715-6723.

Nghiem, Q.H. 2015. GIS-based Spatial Multi-criteria Analysis: A Vulnerability Assessment Model for the Protected Areas of Vietnam

Nohani, E., M. Moharrami, S. Sharafi, K. Khosravi, B. Pradhan, B.T. Pham, S. Lee and A.M. Melesse. 2019. Landslide Susceptibility Mapping Using Different GIS-Based Bivariate Models

Pourghasemi, H.R., B. Pradhan, and C. Gokceoglu, 2012. Application of fuzzy logic and analytical hierarchy process (AHP) to landslide susceptibility mapping at Haraz watershed, Iran. Nat. Hazards, 63, 965–996.

Pourghasemi, H., H. Moradi, and S.F. Aghda. 2013. Landslide susceptibility mapping by binary logistic regression, analytical hierarchy process, and statistical index models and assessment of their performances. Nat. Hazards, 69, 749–779.

Pradhan, B., Lee, S., and Buchroithner, M. F.: Remote Sensing and GIS-based Landslide Susceptibility Analysis and its Cross-validation in Three Test Areas Using a Frequency Ratio Model, Photogramm. Fernerkun., 2010, 17–32, https://doi.org/10.1127/1432-8364/2010/0037, 2010.

Preston, B.L., Yuen, E.J., Westaway, R.M., 2011. Putting vulnerability to climate change on the map: a review of approaches, benefits, and risks.
Sustain. Sci. 6 (2), 177e202. https://doi.org/10.1007/s11625-011-0129-1.

Regmi, A.D., K.C. Devkota, K. Yoshida, B. Pradhan, H.R. Pourghasemi, T. Kumamoto, and A. Akgun. 2014. Application of frequency ratio, statistical index, and weights-of-evidence models and their comparison in landslide susceptibility mapping in Central Nepal Himalaya. Arab. J. Geosci., 7, 725–742.

Saaty, T.L. 1980. The analytic hierarchy process: planning, priority setting, resource allocation. McGraw-Hill International Book Company, New York.

Saaty, T. L. 1990. How to make a decision: The analytic hierarchy process. In: Decision making by the analytic hierarchy process: Theory and applications, 48 (1), 9-26. DOI:10.1016/0377-2217(90)90057-I.

Saaty, T.L. and G. L. Vargas. 2001. Models, Methods, Concepts, and Applications of the Analytic Hierarchy Process, Kluwer Academic Publisher, Boston.

Senouci, R., N.-E., Taibi, A.C. Teodoro, L., Duarte, H. Mansour, and R. Yahia Meddah. 2021. GIS-Based Expert Knowledge for Landslide Susceptibility Mapping (LSM): Case of

Mostaganem Coast District, West of Algeria. Sustainability, 13, 630. https://doi.org/10.3390/su13020630

USGS (United States Geological Survey). 2014. Landslide Types and Processes